PERGAMON

International Journal of Heat and Mass Transfer 45 (2002) 3875–3884

International Journal of HEAT and MASS TRANSFER

www.elsevier.com/locate/ijhmt

Neural network-based prediction of the oscillating behaviour of a closed loop thermosyphon

A. Fichera *, A. Pagano

Dipartimento di Ingegneria Industriale e Meccanica, Università degli Studi di Catania, Viale A. Doria n. 6-95125 Catania, Italy

Received 20 December 2000; received in revised form 18 October 2001

Abstract

The aim of this work is to address the problem of modelling the dynamical behaviour, manifested during unstable operation, of an experimental closed loop thermosyphon. A generalised Nonlinear Auto-Regressive Moving Average with eXogenous inputs (NARMAX) model, implemented by means of neural networks, is used to address the identification of the system dynamics by means of input–output experimental measurements.

A comparison between the experimental measurements and the results both of a mathematical model reported in the literature and of the proposed neural model is presented. Reported results show that the proposed neural model does not suffer of the poor correspondence between simulated and experimental data that affects the mathematical model.

1. Introduction

Reliable and energy-saving cooling of heat sources represents a stringent requirement in many relevant industrial applications. Closed loop thermosyphon are an interesting technical solution both for reliability and for cost reduction, as they are thermo-fluid-dynamical systems in which cooling of a heat source is obtained by circulation of a fluid without the help of mechanical pumping components, and therefore of moving elements. In fact, in such systems the driving force for the fluid motion is determined by density gradients established between the top of the loop, which is cooled, and the bottom of the loop, which is the heat source to be refrigerated.

The absence of pumps drastically reduces the probability of failure in the heat removal from the heat source and eliminates the cost of pumping. This is the main reason for which natural is preferred to forced convection in energy plants in which safety is a stringent requirement, as nuclear power plants, or electrical machine rotor cooling [1–3], or where considerable costs reduction may be obtained, as geothermal plants or solar heaters that are characterised by low temperature thermal source and higher circulating flow rate [4,5]. Finally, natural convection may represent one of the possible technical solution in those systems in which the pumping system cannot be conveniently positioned, such as cooling systems for internal combustion engines, turbine blade cooling or computer cooling [6,7].

The most common configurations reported in the literature are the rectangular [8] and toroidal [9,10] geometries. In both these basic schemes the loop usually lies on a vertical plane, is symmetrical with respect to the vertical axis and consists of a heat source (placed in the bottom and cooled by the circulating flow), a heat sink (placed on top of the loop) in which the circulating flow is cooled; the heat source and the heat sink may be connected or not by adiabatic legs. In particular, the toroidal loops reported in the literature usually lack of adiabatic legs and as they simply consist of two semicircular heat exchanging sections directly connected; whereas rectangular loops, as the one schematised in Fig. 1 and which are the main object of the present study, are usually designed with thermally isolated vertical legs connecting the heat exchanging sections [8] (horizontal adiabatic connection pieces may be present or not).

* Corresponding author. Tel.: +39-095-7382450; fax: +39-095-337994.

E-mail addresses: afichera@diim.unict.it (A. Fichera), apagano@diim.unict.it (A. Pagano).

0017-9310/02/$ - see front matter
PII: S0017-9310(02)00095-9

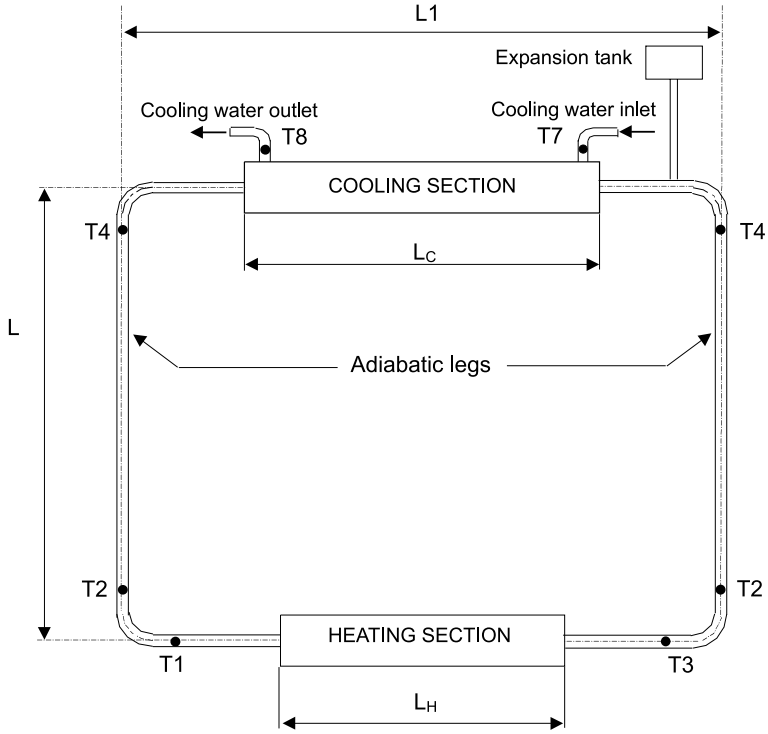

Fig. 1. Scheme of the rectangular natural circulation loop with adiabatic legs used during the experimental phase.

Due to the relevance of their applications, natural circulation loops stability represents a stringent requirement. In fact, the oscillations of the fluid velocity and temperature associated to unstable dynamics are able to compromise the heat removal from the heat source and are, therefore, extremely dangerous for the plant safety.

The occurrence of unstable dynamics mainly depends on the entity of the buoyancy determined by density gradients and, therefore, proportional to the vertical temperature difference. This term depends both on the geometry of the system and on the heating conditions at the boundary. It is just mentioned here that the most common heating conditions considered in literature are symmetrical and consist of: (a) imposed wall temperature [9,11]; (b) imposed heat flux [12,13]; (c) mixed condition [10,14,15].

Forecasting or controlling the oscillations of the process by means of reliable prediction models represents one of the main tasks in the field of natural circulation loops. In particular, early detection of the birth of oscillating behaviours could be useful to determine a suitable control action.

The geometry of the system and the heating conditions at the boundary play a fundamental role in the possibility of modelling such systems. In particular, the governing equations describing the flow inside the loop can be exactly reduced to a three-dimensional dynamical model exhibiting chaotic behaviour only for the toroidal geometry either with known wall temperature or with known heat flux. These models display dynamical behaviours mainly resembling those of the Lorenz system [16]. Conversely, due to the higher complexity such simple models have not been proposed for the cases of mixed conditions or for other geometries. They lack, in particular, for the rectangular geometry with adiabatic legs as the one reported in Fig. 1, which on the other hand represents the most common configuration in real applications.

For this reason the stability of rectangular natural circulation loops was studied by means of a non-linear and distributed parameters mathematical model [1], in which space discretisation of the non-dimensional velocity and temperature was used, leading to a high order non-linear system. The stability of the model was then studied on the linearized model through the construction of a stability map. Anyway, the time evolution of the model variables was not analysed. In their paper Cammarata et al. [8] presented a similar analysis of a natural circulation loop, leading both to the stability map and to the simulation of the system dynamical behaviour. Although suitable to classify the system stability, through the construction of the stability map of the system, the results of this model are affected by a mismatch, mainly

limited to the characteristic frequencies, between experimental and mathematically simulated time-series. Generally speaking, the mismatch between mathematical models and experimental data represents the main limit of scientific works based on this kind of mathematical models.

In this work a different approach, based directly on experimental measurements, was undertaken. The experimental apparatus consisted of a rectangular circulation loop under mixed heating condition; therefore, no exact mathematical model exist for the case study. Chaotic experimental measurements were used as input–output information for a Nonlinear Auto-Regressive Moving Average with eXogenous inputs (NARMAX) model, which was implemented by using Artificial Neural Networks. The obtained model was usefully applied to forecast the birth and the evolution of undesired oscillations. To this aim, the outputs of the Neural Network were recursively fed back to the input layer in order to perform long term predictions. Results show the possibility to effectively address the problem of predicting the temporal evolution of natural circulation loops by means of neural network modeling. This ability will be used to design a controller aiming to avoid unstable behaviours in the loop.

2. Experimental apparatus

Table 1 reports the main dimensions of the experimental natural circulation loop depicted in Fig. 1. It consists of two copper horizontal tubes (heat transfer sections), two vertical phirex tubes, four horizontal phirex tubes and four 90° phirex bends. The lower heating section consists of two independent electrical heating wire, able to provide 0.5 kW each, winding on the outside of the copper tube.

Table 1
Loop main dimensions

Loop height	L	1270 mm
Loop width	L_1	1780 mm
Loop inner diameter	D	26 mm
Heating section length	L_H	800 mm
Cooling section length	L_C	1000 mm

The upper heat extraction system is a coaxial heat exchanger with tap water flowing in the annulus created by an external iron case (diameter 0.2 m). In this way it is possible to impose desired values both of the heat flux in the lower heating section and of the temperature of the coolant. The latter condition can be obtained by adopting high values of the water flow rate so to minimise the temperature difference between the inlet and the outlet of the cooling water. An expansion tank open to the atmosphere is installed on the topmost elevation of the loop allowing the fluid volumetric expansion.

The whole system is equipped with six calibrated (± 0.1 K) T-thermocouples (diameter 1.6 mm) located (see Fig. 1): T2 and T4 on the left vertical tube, T5 and T6 on the right vertical tube and T1 and T3 on the lower horizontal tubes. The thermocouples are connected to a PC that acquires five measurements per second (with a sampling period of 0.2 s) for each of the six thermocouples and then stores only the mean value of these five data. In fact, this results in a sampling period of 1 s and allows high frequency noise components. Hence, the result of each experimental test consists of six time-series corresponding to the temporal evolution of the temperatures measured along the loop. These temperatures will be indicated in the following with the same name of the thermocouples they are measured with.

A set of 16 operating conditions were detected during the experimental tests. Each experimental test was performed starting from the quiet condition, characterised by null temperature difference between any couple of points of the loop and hence by the absence of flow. Therefore all tests are characterised by an initial transient behaviour rapidly evolving towards the regime condition. The experimental grid is reported in Table 2 and indicates the name given to each experiment, which reflects the heat flux and the cooling flow rate imposed at the heat exchanging sections. In particular, each test is indicated by the letter P followed by the heat power value (in kW), a score, the letter Q and the value of the cooling water flow rate (expressed for simplicity in dm^3/min). As an example, the name *P1.8–Q1* refers to the experimental test performed supplying to the heater a heat power $P = 1.8$ kW and using a cooling water flow rate $Q = 1$ dm^3/min. Four values of the cooling water flow rate, Q, were used per each of the four heat power P considered.

Table 2
Experimental test grid

Q (dm^3/min)	Heat power (W)			
	1600	1700	1800	1900
1	*P*1.6–*Q*1	*P*1.7–*Q*1	*P*1.8–*Q*1	*P*1.9–*Q*1
4	*P*1.6–*Q*4	*P*1.7–*Q*4	*P*1.8–*Q*4	*P*1.9–*Q*4
15	*P*1.6–*Q*15	*P*1.7–*Q*15	*P*1.8–*Q*15	*P*1.9–*Q*15
30	P1.6–*Q*30	*P*1.7–*Q*30	*P*1.8–*Q*30	*P*1.9–*Q*30

It is just mentioned here that the experimental time-series that were detected during the test have been shown to be governed by chaos [17]. More in detail, the experimental apparatus may undergo chaotic behaviours characterised by two kinds of attractors: the first appears quite similar to the typical attractor of the Lorenz system (in particular, with two lobes), whereas the second is characterised by a single lobe attractor quite similar to that reported in [18].

3. NARMAX model

The complexity of the exact form of the mathematical description of any real-world system often causes the inability to determine an accurate model. For this kind of systems, input–output models offer a powerful mean to the identification of the system within a certain accuracy and with reasonable computational cost. in the present contest the possibility to apply a *Multiple Linear Regression* for the identification of the system dynamics was not considered; in fact, the chaotic nature of the experimental time-series pointed out the necessity to choose a non-linear identification approach.

The *NARMAX* model was shown to be a general class of non-linear input–output models [19] and provides a straightforward way to represent with adequate approximation a large class of non-linear systems. In mathematical terms, a NARMAX performs the identification of a system in terms of a non-linear functional expansion of lagged inputs and outputs. In other words, the identification of a non-linear system is based on the characterisation of its output $y(k)$ at a given instant k, by means of the application of the non-linear function F to the inputs and outputs in the previous time-steps. Therefore, considering for simplicity a Single Input–Single Output (SISO) system, $y(k)$ can be expressed as:

$$y(k) = F[y(k-1), \ldots, y(k-n_y), u(k-1), \ldots, u(k-n_u)], \tag{1}$$

where $u(\cdot)$ is the input at the generic time sample.

It has been demonstrated that a NARMAX model is able to represent a discrete time invariant non-linear system in a region around an equilibrium if the system has lumped parameters and it can be represented by a linearized model in a neighbourhood of the equilibrium [20].

A common way to built a *generalised* NARMAX model (i.e. valid for different equilibria and even for piecewise linear function F) is to use a *Multi Layer Perceptron Neural Network*, which does not require the linearisation around equilibria. The high potentials, flexibility and easiness of use of neural networks in modelling and pattern recognition problems is well known and a good review of their applications to energy systems is reported in [21].

In the present contest they were used to implement a generalised form of the NARMAX model (1). In fact, whereas the existence conditions of a NARMAX model are locally valid and the function F is assumed to be continuous and differentiable, the approximation of the non-linear function F through combination of sigmoidal functions, as that performed by a neural network, is valid also for piecewise continuous functions and in wider region of state space. Hence, if a dynamical system needs various NARMAX models to be represented in different regions of state space, separated by discontinuity points, then a single neural network [19] is able to interpolate the system dynamical behaviour for different region of state space. The greater flexibility offered and the wide number of operating conditions detected during the experimental phase (corresponding to different regions of state space) make the neural network approach suitable for the aim of this work. As well known, neural network used for function approximation are feed-forward networks with one or more hidden layers between the input and the output, each layer being formed by simple computing units, called nodes or neurons. The input–output relationship of the jth hidden node can be expressed [22] as:

$$\mathrm{out}_j = a\Big(\sum w_{ij}\mathrm{in}_i + \mu\Big), \tag{2}$$

where in_i is the ith input to the node (i.e. the output of the ith node of the antecedent layer), out_j is the node output, w_{ij} are the weights connecting the jth node to the nodes of the antecedent layer, μ is a threshold parameter and $a(\cdot)$ is the node activation function. For simplicity, the weights of a neural network are indicated collected into a matrix W.

For a neural network with n inputs and m outputs, the global input–output relationship is a function $NN : R^n \to R^m$. During the training of the network, the model receive some input vectors and the output is compared with desired targets corresponding to these inputs. The weights w_i connecting the nodes are recursively updated, according to a specified training algorithm, in order to minimise a cost function that generally speaking coincides with the prediction error, evaluated as the difference between the desired output (i.e. the target) and the actual output of the network. At the end of training the function $NN : R^n \to R^m$ is determined. Cybenko demonstrated that NN can uniformly approximate any continuous function $F : D \subset R^n \to R^m$, where D is a compact subset of R^n [23,24]. This ensures that the function F in (1) can be approximated by a neural network, so that:

$$y(k) \approx NN[y(k-1), \ldots, y(k-n_y), u(k-1), \ldots, u(k-n_u)]. \tag{3}$$

In this paper, the neural approach was used in order to predict the time evolution of the system in study. The structure of the neural model was chosen according to some basic consideration on the process and on the knowledge achieved on the mathematical model. In fact, the system is represented by a set of first-order differential equations in which the number of state variables depends on the discretisation adopted. Although the system is theoretically infinite dimensional, for control purposes even a low number of variables is able to give an accurate representation of the system dynamics. In particular, the cooling water flow rate at the cooling section, Q, and the heat power at the heating section, P, are the inputs to the system and completely define each operating condition. The system outputs herein chosen are the inlet–outlet temperature differences at the cooling and heating sections, calculated as the differences between the measures of thermocouples T4 and T6 and between thermocouples T2 and T5, indicated in the following respectively as ΔT46 and ΔT25, and the temperature difference ΔT24, between the measures of thermocouples T2 and T4 placed on the vertical leg. These three variables were considered sufficient as: ΔT46 and ΔT25 give information on the changes occurring to the fluid in its passage through the heat exchanging sections and ΔT24 is proportional to the buoyancy, and hence is related to the flow driving term. With this choice of the inputs and outputs, the model structure is closely related to the underlying process and its final representation can be easily understood. Adapting the general formula (3) to the present case, the input–output relation defining the model can be expressed as:

$$[\Delta T25(k)\Delta T46(k)\Delta T24(k)] = NN[\Delta T25(k-1), \Delta T46(k-1), \Delta T24(k-1), Q, P]. \quad (4)$$

The vectors of the input and output data sets were initially normalised in the range $[-1, 1]$ so as to allow better performances of the neural model. Considering the slow dynamics of the system, a lower sampling rate has been adopted, i.e. the data set was decimated considering one out of five data with a sampling period of 5 s.

Fig. 2 reports a schematic of the structure of the neural network herein used. In the figure, $\sum$ simply indicates the generic neuron, performing the generic transformation described in (2) to the weighted sum of its inputs. As the figure shows, the neural network was made of three layers: an input layer of five neurons that simply receives the model inputs, a hidden layer of nonlinear neurons (implementing the *tangent-sigmoid* function) and an output layer with three linear neurons (implementing the *pureline* function).

The number of neurons of the hidden layer was chosen increasing it until the network was able to guarantee good performances and a further increase was not effective or even worsening.

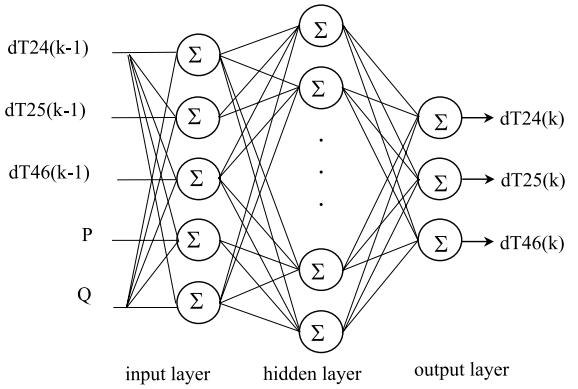

Fig. 2. Scheme of the neural network.

In order to chose on an analytical base the performances of the model, the properties of the error of the model, defined as the difference between experimental and simulated time-series, where considered. In general, the prediction of a model are satisfactory when the error has the same characteristic of a *white noise*, i.e. it has zero mean and it is uncorrelated [22]. It is therefore necessary to verify that the autocorrelation function of the normalised error $\varepsilon(t)$, namely, assumes the values 1 for $t = 0$ and 0 elsewhere; in other words, it is required to the function to behave as an impulse. This condition is, of course, ideal and in reality it is usually sufficient [22] to verify that $\phi_{\varepsilon\varepsilon}(t)$, remains in a confidence band usually fixed at the 95%, which means that $\phi_{\varepsilon\varepsilon}(t)$ must remain inside the range $\pm 1.96/\sqrt{N}$ (with N number of data on which $\phi_{\varepsilon\varepsilon}(t)$ is calculated).

The neural network was trained using the Levenberg–Marquardt rule [25], according to which the matrix of the weights of the network is updated on the base of the Jacobian matrix, J, collecting the partial derivatives of the error of the network e with respect to the weights. In other words, the matrix ΔW collecting the corrections of the weights in matrix W is computed according to:

$$\Delta W = (J^{\mathrm{T}}J + \alpha I)^{-1} J^{\mathrm{T}} e. \quad (5)$$

The training set was made choosing four quite different oscillations, in order to be well representative of the possible system behaviours, for each of the three time-series used as inputs per each experimental operating condition. More in detail, about 150 pattern-target couples per each operating condition were used during the neural network training, constituting a training set of 2200 couples, which were previously randomised.

The number of epochs used during the training was not constant for all the neural networks. This was due to

the adoption of a strategy for the prevention of overfitting. In particular, during the training, each neural network was contemporary tested using a testing data set, whose elements were not used for updating the neural network weights. The criterion and the dimension (2000 pattern–target couples) for the creation of this data set was the same used for the creation of the training set. This technique avoids overfitting in that it can stop the training when testing performances get worse from one epoch to the following.

The number of training epochs was indeed much lower (of about two orders of magnitude) than the number of epochs usually required from the traditional back-propagation rule, as a consequence of the very fast convergence ensured by the chosen training rule; in fact, it ranged from 32 to 65 which is very.

After this phase, each neural network was tested in order to validate the model error. This was done using a further set, called validation set, which was created analogously to the previous sets but considering a sensibly higher number of pattern–target couples (about 15,000), which were different from those considered in the other two sets.

Table 3 synthesises the performance of the various networks implementing the NARMAX model (4). From the table it is apparent that the best performances where obtained using ten neurons, which ensured the lowest error (both in terms of the mean value, very close to zero, and of the mean absolute value).

The first plot in Fig. 3 shows one of the actual output of the system, the temperature difference ΔT25 detected during operating condition *P1.8–Q1*, and the corresponding neural network output obtained simulating the neural network with pattern–target couples from the validation set. Note that the experimental time-series is chaotic, as it was demonstrated in [17] and can be intuitively perceived by the differences in the maximum values of the oscillations, which point out the non-periodicity of the phenomenon.

The second plot of the same figure reports the autocorrelation function, $\phi_{\varepsilon\varepsilon}(t)$, of the prediction error calculated over a subset of 100 step of the neural network (corresponding to a prediction of 500 s) for the same data.

Both these plots evidence that the neural network predictions are satisfactory and indicate that the training was sufficiently wide and ensured adequate generalisation properties. In fact, it is apparent from the comparison the good fitting of the simulated time-series with the experimental chaotic one and it is also evident that it is verified that the autocorrelation function remains bounded in the range $\pm 1.96/\sqrt{N}$ (indicated by the dashed lines).

Fig. 4 reports the results obtained for another operating condition (*P1.9–Q1*), where the system manifest a kind of chaotic motion morphologically similar to that typical of Lorenz chaos. It can be seen that also in this case the neural network performs satisfactorily the prediction of the temperature difference ΔT25, and is therefore able to adequately generalise the various possible system dynamics.

The results for the other two outputs of the system and for the whole set of remaining operating conditions are perfectly consistent with those presented in Figs. 3 and 4.

Moreover, the neural model was used in the prediction scheme reported in Fig. 5 in order to verify its ability to describe autonomously the time evolution of the system variables. It is just mentioned here that other methodologies might ensure more reliable prediction performances; nonetheless, they were not tested as the adopted scheme was applied only in order to test in a simple way the possibility to extend the model prediction. The scheme, in which $\Delta T = [\Delta T25, \Delta T46, \Delta T24]$ and the star indicates the output simulated by the neural model, describes the following steps:

- at the generic time $k - q$, the neural network receives as input the actual measurement $\Delta T(k - q)$ and predicts the corresponding output $\Delta T(k - q + 1)^*$;
- the next $q - 1$ inputs to the model are the output of the model itself in the previous steps with the addition of the heat power and of the cooling flow rate; in this way, the output of the model at generic time

Table 3
Neural networks performances

Number of neurones (%)	Neural network performances		
	Mean prediction error (%)	Mean absolute prediction error (%)	Uncorrelated error (%)
4	0.827	5.2	No
6	0.258	3.9	No
8	0.076	2.8	Yes
10	0.009	1.7	Yes
12	0.014	1.9	Yes
14	0.016	1.8	Yes

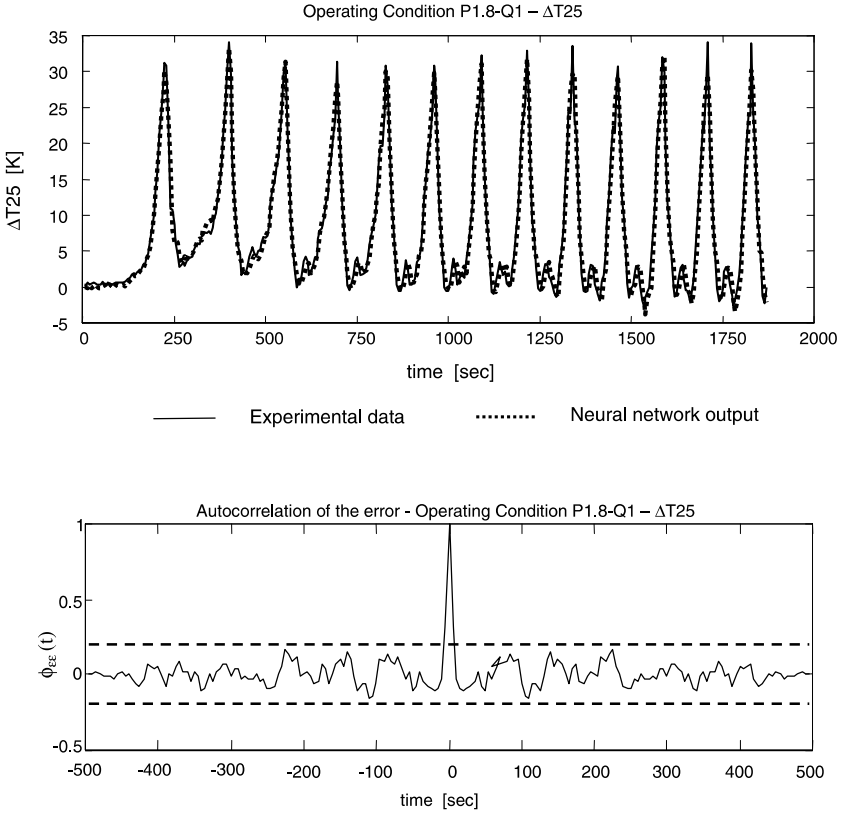

Fig. 3. Comparison between the experimental and neural network simulated time series ΔT25 for operating condition *P1.8–Q1* (first plot); autocorrelation function of the prediction error (second plot).

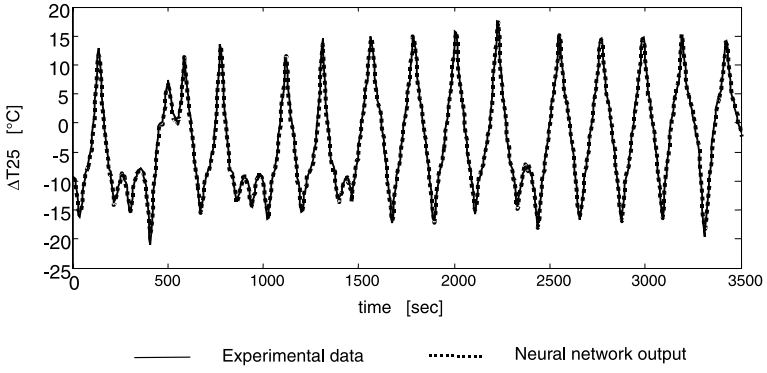

Fig. 4. Comparison between the experimental and neural network simulated time-series ΔT25 for operating condition *P1.9–Q1*.

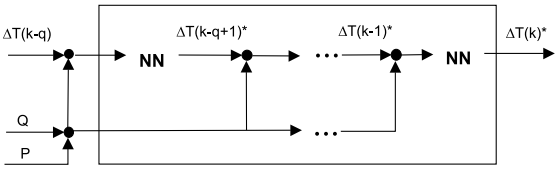

Fig. 5. Recursive prediction scheme.

k is predicted from the actual output of the system at time $k - q$;

Fig. 6 reports the mean prediction errors on the neural model outputs plotted versus the number of prediction steps q. In the figure Err($\Delta T25$), Err($\Delta T46$) and Err($\Delta T24$) are calculated as absolute differences of

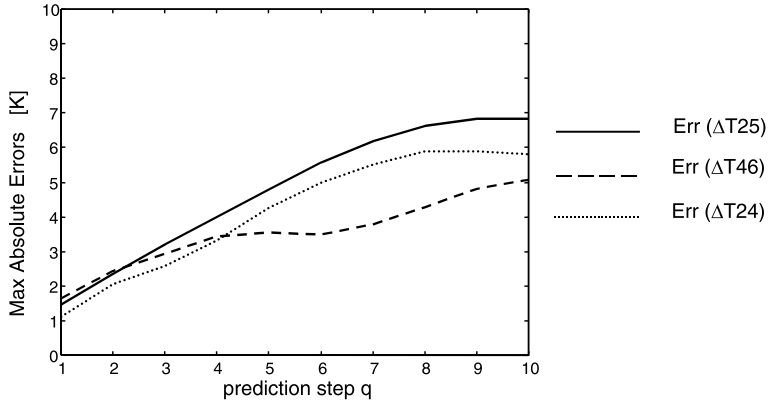

Fig. 6. Mean absolute prediction errors versus number of prediction steps q.

the actual and the simulated values, respectively, of temperature difference $\Delta T25$, $\Delta T46$ and $\Delta T24$.

The analysis of the figure points out that the recursive prediction seems to be sufficiently reliable, though depending on the specific application, up to five steps whereas it looses its validity for a higher number of steps. In fact, as it was expected due the chaotic nature of the system, the mean value of the error progressively increases with the number of prediction steps, until it reaches a sort of saturation value where predictions are clearly unreliable.

In Fig. 7 comparisons between the actual output and the three and five steps ahead predictions are, respectively, reported. It must be noticed that for $q = 3$ (corresponding to a prediction step of 15 s) the simulated time-series satisfactory approximates the experimental data. For $q = 5$ (prediction step of 25 s) the approximation is of course slightly worse; nevertheless, the

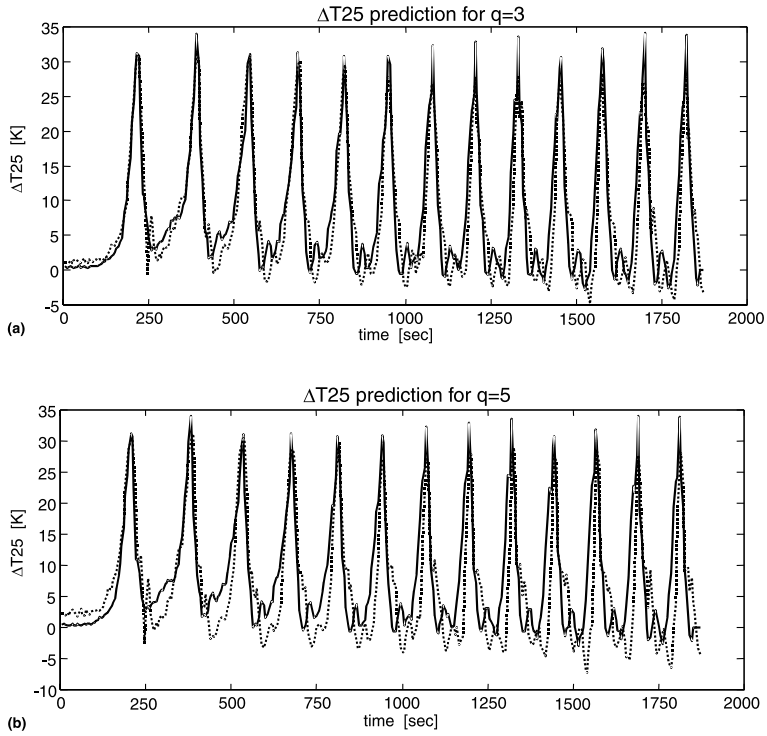

Fig. 7. Simulated and actual output for the condition *P1.8–Q1* for: (a) $q = 3$ and (b) $q = 5$.

model is still able to reveal the occurrence of the dominant patterns of the oscillations and therefore can be used in the design of a control system.

This observation is useful to point out that the optimal choice for q may depend on the specific application of the predictive model.

4. Conclusion

In this paper the identification of the chaotic dynamics of a closed loop thermosyphon was addressed by means of a generalised NARMAX model, which was obtained by means of a neural network. The input to the model were chosen in order to obtain a model structure closely resembling the underlying process and a final representation easily understandable. In particular, they were the inlet–outlet temperature differences at the cooling and heating sections, the vertical temperature difference, the cooling water flow rate at the cooling section, and the heat power at the heating section. The model outputs are the one step ahead prediction of the temporally varying inputs (i.e. the three temperature differences). Results of the simulations show that the model is able to give a satisfactory one-step ahead predictions of the experimental chaotic time-series and that the chosen neural network methodology has been able to perform correct predictions even in absence of appropriate governing equations. Moreover, the developed neural model was used in a recursive scheme in order to test its ability to perform longer term predictions. In this way, the predictive capability of the neural model was tested and it was shown that satisfying predictions were obtained, at least for a few steps ahead (due the chaotic behaviours of the system). These are interesting results as they point out the potential application of the neural model herein presented to a control scheme. In fact, the possibility to design a neural controller is actually under study.

As a final remarks it is useful to point out that, though the validity of the proposed model is limited to the experimental set-up on which input–output measurements were detected, it is the methodology itself that has a very high potential and that can be exported very easily to other systems, independently from their geometrical configuration, scale and heating conditions.

References

[1] P.K. Vijayan, A.K. Nayak, D.S. Pilkhwal, D. Saha, V. Venkat Raj, Effect of loop diameter on the stability of single-phase natural circulation in rectangular loops, in: Proceedings of the Fifth International Topical Meeting on Reactor Thermal Hydraulics (NURETH-5), Salt Lake City, vol. 1, 1992, pp. 261–267.

[2] J. Miettinen, T. Kervinen, H. Tomisto, H. Kantee, Oscillations of single-phase natural circulation during overcooling transient, in: Proceedings of the ANS Topical Meeting, Atlanta, vol. 1, 1987, pp. 20–29.

[3] R. Greif, Y. Zvirin, A. Mertol, The transient and stability behavior of a natural convention loop, Trans. ASME 101 (1979) 684–688.

[4] D.B. Kreitlow, G.M. Reistad, C.R. Miles, G.G. Culver, Thermosyphon models for downhole heat exchanger applications in shallow geothermal systems, ASME J. Heat Transfer 100 (1978) 713–719.

[5] Y. Zvirin, A. Shitzer, A. Bartal-Bornstein, On the stability of the natural circulation solar heater, in: Proceedings of the Sixth International Heat Transfer Conference, Toronto, vol. 20, 1978, pp. 997–999.

[6] Y. Zvirin, A Review of N.C. Loops in PWR and other systems, Nucl. Eng. Des. 67 (1981) 203–225.

[7] D. Japikse, in: Advances in Thermosyphon Technology, in: T.F. Irvine, in: J.P. Harnett (Eds.), Advances in Heat Transfer, vol. 9, 1973, p. 111.

[8] G. Cammarata, A. Fichera, M. Froghieri, M. Misale, M.G. Xibilia, A new modelling methodology of natural circulation loop for stability analysis, in: Proceedings of Eurotherm Seminar No. 63, Genova, 1999, pp. 151–159.

[9] Y.-Z. Wang, J. Singer, H.H. Bau, Controlling chaos in a thermal convection loop, J. Fluid Mech. 37 (1992) 479–498.

[10] J. Singer, Y.-Z. Wang, H.H. Bau, Controlling a chaotic system, Phys. Rev. Lett. 66 (9) (1991) 1123–1125.

[11] M. Sen, E. Ramos, C. Trevino, O. Salazar, A one-dimensional model of a thermosyphon with known wall temperature, Int. J. Heat Fluid Flow 8 (3) (1987) 171–181.

[12] M. Sen, E. Ramos, C. Trevino, The toroidal thermosyphon with known heat flux, Int. J. Heat Mass Transfer 28 (1) (1985) 219–233.

[13] M. Sen, E. Ramos, C. Trevino, O. Salazar, The effect of axial conduction on a thermosyphon with prescribed heat flux, Eur. J. Mech., B-Fluids 8 (1) (1989) 57–72.

[14] M. Gorman, P.J. Widman, K.A. Robbins, Nonlinear dynamics of a convection loop: a quantitative comparison of experiment with theory, Physica 19D (1986) 255–267.

[15] P.J. Widman, M. Gorman, K.A. Robbins, Nonlinear dynamics of a convection loop II: Chaos in laminar and turbulent flows, Physica D 36 (1989) 255–267.

[16] E.N. Lorenz, Deterministic nonperiodic flow, J. Atmos. Sci. 20 (1963) 131–141.

[17] A. Fichera, M. Froghieri, A. Pagano, Comparison of the dynamical behaviour of rectangular natural circulation loops, Process Mech. Eng. J., Part E 215 (2002).

[18] J.A. Yorke, E.D. Yorke, J. Mallet-Paret, Lorenz-like chaos in a partial differential equation for a heated fluid loop, Physica 24D (1987) 279–291.

[19] S. Chen, S.A. Billings, P.M. Grant, Representations of non-linear system: the NARMAX model, Int. J. Control 49 (5) (1989) 1013–1032.

[20] I.J. Leontaritis, S.A. Billings, Input–output parametric models for nonlinear systems Part I: Deterministic nonlinear systems, Int. J. Control 41 (2) (1985) 303–328.

[21] S.A. Kalogirou, Applications of artificial neural networks for energy systems, Appl. Energy 67 (1 and 2) (2000) 17–35.

[22] S. Chen, S.A. Billings, P.M. Grant, Non-linear system identification using neural networks, Int. J. Control 51 (6) (1990) 1191–1214.
[23] G. Cybenko, Approximation by superpositions of a sigmoidal function, Math. Control Signals Syst. 2 (1989) 303–314.
[24] K. Funahashi, On the approximate realization of continuous mapping by neural networks, Neural Networks 2 (1989) 183–192.
[25] P.T. Boggs, R.H. Byrd, R.B. Schnabel, A stable and efficient algorithm for nonlinear orthogonal distance regression, SIAM J. Sci. Statist. Comput. 8 (1987) 1052–1078.